JOURNAL OF MATERIALS SCIENCE 24 (1989) 892–898

Crystallization of gel-derived alumina and alumina–zirconia ceramics

I. M. LOW*, R. McPHERSON
Department of Materials Engineering, Monash University, Clayton 3168, Victoria, Australia

The crystallization behaviour and phase relations in gel-derived alumina and alumina–zirconia ceramics has been investigated. Zirconia was found to form a limited metastable solid solution with the alumina matrix. When present in solid solution, zirconia phase appeared to enhance rapid growth of corundum grains. There was no apparent grain refinement in the alumina–zirconia composites. The implications of microporous gel structures on the modification of microstructures in these gel-derived ceramics are discussed.

1. Introduction

Corundum is the only stable phase in alumina ceramics. These ceramics may be prepared by either thermal decomposition of aluminium hydroxides and salts [1] or by rapid quenching of alumina melts [2, 3]. Recent works have indicated that gels are excellent alternative materials for making alumina ceramics as well as alumina–zircona composites.

Becher [4] prepared alumina–zirconia composites from gels and observed significant improvement in fracture toughness and the thermal shock resistance. Similar observations were also reported by various investigators on these ceramics made by the conventional mixing and compaction technique [5–9]. In addition to improvement in toughness and strength, dispersion of fine metastable zirconia particles in the matrix of alumina has been found to hinder the abnormal coarsening of alumina grains [10, 11]. Another elegant technique of making alumina–zirconia ceramics is by chemical vapour deposition (CVD) [12, 13]. Other possible methods include: (i) hydrothermal oxidation [14] and (ii) melt quenching [15].

Cr_2O_3 has been well established to form a solid solution with alumina [2]. Other compounds such as Na_2O, MgO, NiO and Li_2O have also been observed to form solid solutions with Al_2O_3 [16, 17]. No values have been published on the solid solution of zirconia in alumina although a considerable amount of work has already been done on this composite. As in mullite–zirconia composites and most ceramics, the solubility of zirconia in alumina is expected to be limited.

It is the aim of this paper to report results obtained from the crystallization of gel-derived alumina and alumina–zirconia ceramics as well as to investigate the extent and the mechanism of this solid solution formation. The effect of dispersed zirconia (up to 20 wt %) on the microstructure of alumina matrix was also studied.

2. Experimental procedures

Commercial purity zirconium chloride and laboratory prepared aluminium isopropoxide [18] were used as starting materials for the preparation of gels. Initially, the chemicals were mixed in a plastic cup containing carbon tetrachloride as a solvent and diluted with some dry ethanol. The resultant solution was immersed in a chilled solution for 0.5 h before hydrolysis. The latter was done by dropwise addition of water under vigorous stirring. This *in situ* process of preparing the alumina–zirconia gel allows high homogeneity to be achieved and prevents premature hydrolysis of zirconium tetraethoxide. Upon completion of hydrolysis, a plastic film with several holes was used to seal the cup and the solution was allowed to gel over a period of several days in a constant humidity oven in which the temperature was increased in steps from 40 to 80° C.

Differential thermal analysis (DTA) of the gel was performed with a Rigaku Micro DTA apparatus. A heating rate of $10° C min^{-1}$ was used. Characterization of the crystalline phases formed in heat-treated gels was done with a Philips X-ray Diffractometer (PW 1050/25 wide-angle goniometer). Nickel-filtered Cu$K\alpha$ radiation was used. Finely ground gel powder was placed on an aluminium disc as a substrate.

The specimens for the infrared analysis were prepared by the pellet method. The gel powder was mixed with KBr (gel to KBr ratio of 1:250) and pressed into a thin disc. A reference pellet of KBr was also used. Infrared spectra of gels were recorded on a Pye-Unicam SP3-200 spectrometer.

Transmission electron microscopy of gels was done by direct observation of finely ground gel powder which was placed on a 400 mesh copper grid.

3. Results

Petrographic phase analyses of alumina and alumina–zirconia ceramics are shown in Table I. The results indicate that prior to the formation of corundum, metastable phases of γ and θ alumina were formed at lower temperatures. In contrast to mullite–zirconia ceramics, the results in Table I suggest that the metastable solubility limit of zirconia in corundum at

* *Present address*: Department of Materials Engineering, Curtin University of Technology, GPO Box U 1987, Perth 6001, Australia.

0022–2461/89 $03.00 + .12

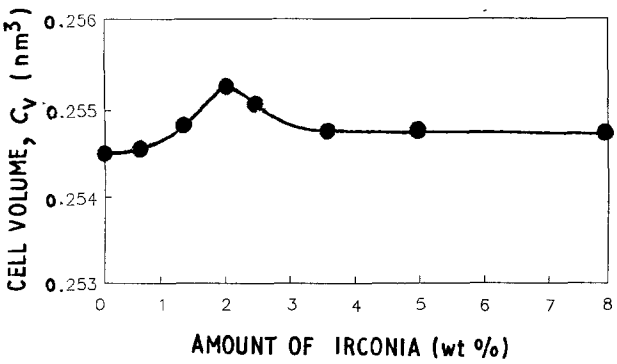

Figure 1 Variation of cell volume of corundum with the amount of zirconia.

1300° C was between 1.5 and 2.0 wt %. This value is substantiated by the cell dimension measurements as a function of the amount of zirconia added (Fig. 1). The value of this metastable solubility limited as computed graphically is about 1.85 wt % zirconia at 1300° C. A perusal of the results in Table I also reveals that this value decreases with increasing temperature and heating time and vice versa. For temperatures below 1200° C, the solubility limit was slightly over 2 wt % zirconia. It is doubtful if the metastable solubility of zirconia in corundum would extend to 5 wt % although it may be true in the metastable γ alumina which is a spinel with significant crystal defects. For alumina–zirconia ceramics, the monoclinic zirconia particles were observed to crystallize at lower temperatures than those in mullite–zirconia composites [19]. Apparently, the alumino–silicate matrix has a better stabilization effect on the metastable zirconia particles than the pure alumina matrix.

Perusal of the results in Table I also suggests that the transformation temperature of transitional aluminas to α-Al_2O_3 appeared to be affected by the addition of ZrO_2. For instance, γ-Al_2O_3 transformed to α-Al_2O_3 at 1150° C when 2 wt % was added instead of 1300° C in pure Al_2O_3. However, θ-Al_2O_3 appeared to persist at higher temperatures when ZrO_2 (1.5 and 2.0 wt %) was introduced.

The DTA curves of pure alumina and its composites are shown in Fig. 2. There were no apparent exotherms to be associated with the crystallization of γ, θ and α alumina or tetragonal zirconia. The latter was only apparent for zirconia contents greater than 10 wt % [20]. These observations are inconsistent with the thermal behaviour of the alumina gel prepared by Yoldas [21] who obtained a sharp exothermic peak at about 1200° C in the DTA curve which corresponded to the transformation of δ- to α-Al_2O_3. The endotherms were attributed to the dehydration and the dehydroxylation of gels and residual alkoxides, respectively.

The infrared spectra of the evolution of alumina gel to crystalline aluminas (α and γ) are depicted in Fig. 3. The spectrum of the gel produces a sharp band at about 1050 cm^{-1} which corresponds to the absorption of Al–OH groups. The broad band at around 610 cm^{-1} is characteristic of six-coordinated aluminium ions. The spectrum of γ-Al_2O_3 is very different from that of the gel. Most of the Al–OH groups were eliminated and in addition to the presence of six-fold coordination aluminium ions, there is a large proportion of aluminium ions with four-fold coordination (800 and 690 cm^{-1}) which are characteristic of disordered alumina structures containing tetragonally coordinated aluminium sharing corners and edges [22]. When aluminium ions are in four-coordination, they exert a stronger electrical field on surrounding oxygens than in the case of six-coordination aluminium [21], causing the absorption bands to become more diffuse. Virtually all the aluminium ions in α-Al_2O_3 are in six-fold coordination which is consistent with the hexagonal close-packed structure of corundum. From ^{27}Al magic angle spinning nuclear magnetic resonance (MASNMR) studies on alumina gels, Komarneni and Roy [23] observed partial conversion of octahedral aluminium to tetrahedral aluminium when the gel was heat treated at 500° C. These observations suggest that aluminium ions are capable of exhibiting both four- and six-fold coordinations and the conversion from one form to the other can occur readily.

The effect of dispersed zirconia on the grain size of

TABLE I Petrographic phase analyses of Al_2O_3 and Al_2O_3–ZrO_2 ceramics

Temperature (° C)	Amount of ZrO_2 (wt %)					
	0	0.5	1.5	2.0	3.5	⩾8
600	A	A	A	A	A	A
875	γ_s	γ_s	γ_s	γ_s	γ_m, TZ_w	γ_m, TZ_w
950	γ_s	γ_s	γ_s	γ_s	γ_m, TZ_w	γ_m, TZ_m
1000	γ_s	γ_s	γ_s	γ_s, θ_w	α_t, γ_m, TZ_w	γ_m, TZ_m
1150	γ_s, θ_m	γ_s, θ_m	α_w, γ_m, θ_m	α_m, θ_m	α_m, θ_m γ_m, TZ_w	γ_m, θ_w TZ_m, MZ_w
1200	γ_m, θ_m	α_m, θ_w	α_m, θ_w	α_m, θ_m, TZ_t	α_m, θ_m, TZ_m	α_s, θ_w TZ_m, MZ_m
1300	α_s	α_s	α_s, θ_w	α_s, θ_w, TZ_t	α_s TZ_m, MZ_w	α_s TZ_s, MZ_s
1400	α_s	α_s	α_s, TZ_t	α_s TZ_w, MZ_t	α_s TZ_m, MZ_m	α_s TZ_s, MZ_s
1500	α_s	α_s TZ_t, MZ_t	α_s TZ_w, MZ_t	α_s TZ_m, MZ_w	α_s TZ_m, MZ_m	α_s TZ_s, MZ_s

γ, θ, α: γ–, θ–, α–Al_2O_3. A = amorphous.
TZ, MZ, Tetragonal and Monoclinic Zirconia, respectively.
s = strong, m = medium, w = weak, t = trace.

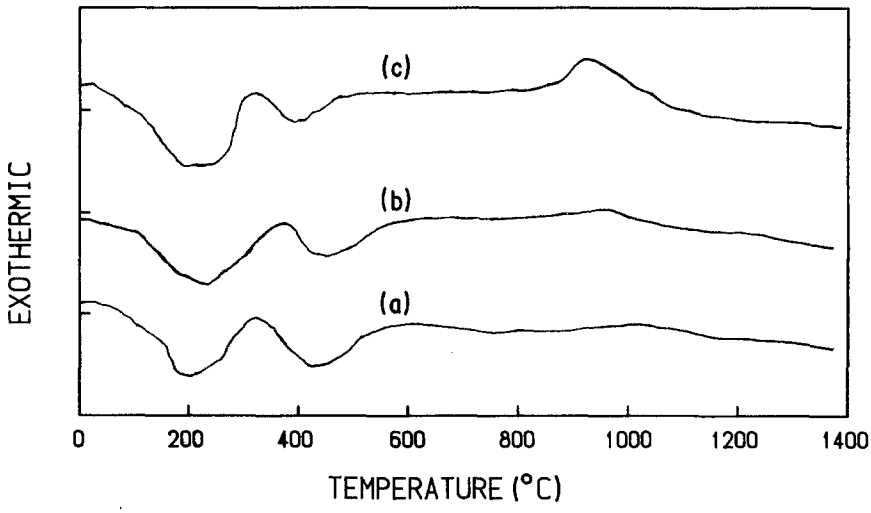

Figure 2 DTA curves of alumina and alumina–zirconia gels. (a) Al_2O_3; (b) < 3 wt % ZrO_2; (c) > 10 wt % ZrO_2.

corundum at 1300° C is depicted in Fig. 4. As in mullite–zirconia ceramics, there was a considerable enhancement of grain growth in alumina ceramics with zirconia contents in the range of solid solution. No apparent grain growth or grain refinement was observed for these ceramics with zirconia contents outside the range of solid solution at 1300° C. The Arrhenius plot of corundum grain size against reciprocal temperature (Fig. 5) indicates that the presence of up to 8 wt % dispersed zirconia in corundum matrix has no inhibition on grain growth at high temperatures. The peculiar behaviour of initial grain size reduction as exhibited in the ceramic with 1.5 wt % zirconia (Fig. 5) is attributed to the crystallization of tetragonal zirconia which brought about an initial arrest in grain growth. At higher temperatures, this grain growth arrest was nullified, indicating a strong dependence of grain growth on temperature.

The evolution of an alumina gel with increasing temperatures has been observed by electron microscopy. Extremely fine microstructures present in the gel were retained at relatively high temperatures. No distinction can be noticed in the gel before and after the crystallization of γ-alumina, indicating that the process of evolution probably involves the maintenance of chemical, structural and compositional continuity of the phases formed. Fig. 6 depicts the ultrafine microstructure of an alumina gel at various temperatures. A microstructure of an alumina-zirconia composite is shown in Fig. 7.

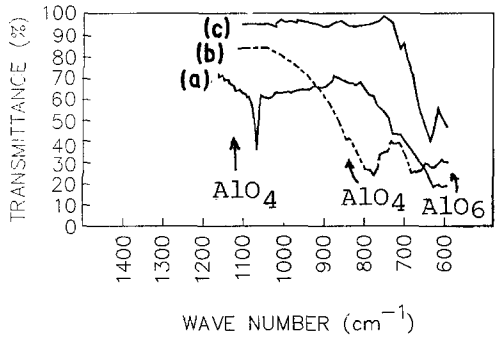

Figure 3 Infrared spectra of evolution of alumina gel to corundum. (a) Alumina gel at ambient temperature; (b) alumina gel heated at 900° C; (c) alumina gel heated at 1500° C.

4. Discussion

4.1. Phase relations in alumina gels

Aluminium alkoxide, $Al(OR)_3$, is readily hydrolysed in water with the formation of aluminium mono- or tri-hydroxide depending on the history of hydrolysis [21]. When hydrolysis is performed in hot water, a stable crystalline monohydroxide forms. In cold water, the hydrolysis results initially in the formation of largely amorphous monohydroxide which may subsequently convert to trihydroxide, bayerite, in its mother liquor unless certain steps are taken [24]. Only monohydroxide forms can be peptized to a clear solution for preparation of non-particulate gels. Dehydration of such gels usually produces amorphous aluminas of extremely small particle size and large surface area. Upon calcination, metastable aluminas of various forms crystallize as intermediates prior to the formation of the stable corundum phase. The sequence of transition of these metastable phases are dependent on the parent phases used and preparation process adopted. For instance, the sequence of phase transformations in alumina melts either during cooling or subsequent heat treatment is

$$\gamma\text{-}Al_2O_3 \rightarrow \delta\text{-}Al_2O_3 \rightarrow \theta\text{-}Al_2O_3 \rightarrow \alpha\text{-}Al_2O_3$$

This sequence of transition is more complex during the thermal decomposition of aluminium hydroxides

$$\text{Bayerite } (Al_2O_3 \cdot 3H_2O) \begin{cases} \rightarrow \eta \rightarrow \theta \rightarrow \alpha \\ \rightarrow \gamma \rightarrow \delta \rightarrow \theta \rightarrow \alpha \\ \rightarrow \text{Boehmite} \end{cases}$$

$$\text{Gibbsite } (Al_2O_3 \cdot 3H_2O) \begin{cases} \rightarrow (Al_2O_3 \cdot H_2O) \\ \rightarrow \chi \rightarrow \kappa \rightarrow \alpha \end{cases}$$

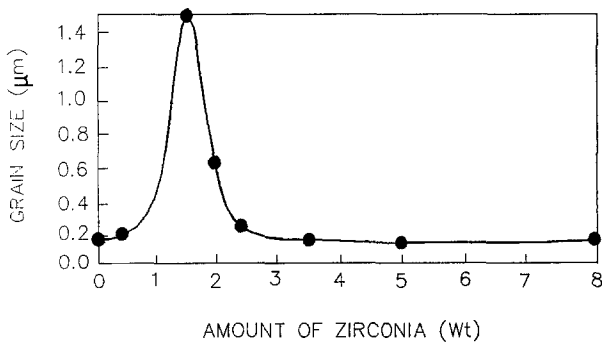

Figure 4 Variation of grain size of corundum as a function of zirconia content heat treated at 1300° C.

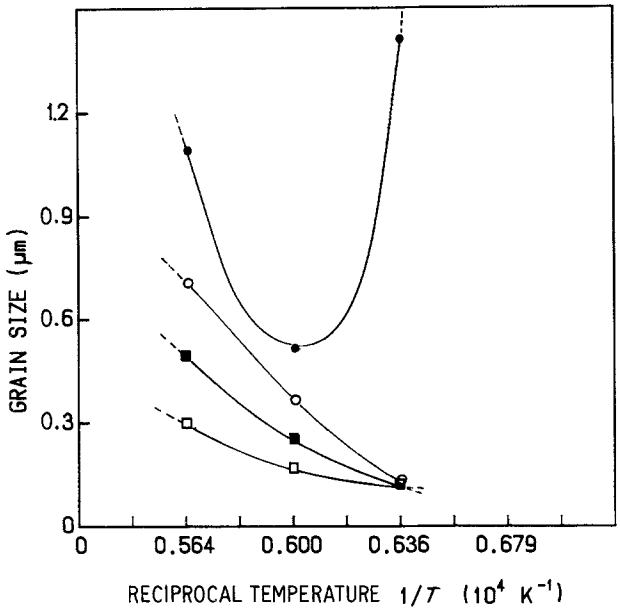

Figure 5 Arrhenius plot of corundum grain size against reciprocal temperature. (□) Pure Al_2O_3; (■) +20 wt % ZrO_2; (○) +8 wt % ZrO_2; (●) 1.5 wt % ZrO_2.

Meanwhile, the metastable phases in the alumina ceramics prepared by chemical vapour deposition are δ and θ [13]. These transformations have attracted an enormous amount of attention, particularly with systems in which the nucleation step has not been controlled [25]. However, the characterization of these transformations is still enigmatic. Numerous hypotheses have been advanced to account for the complex transformation of transitional aluminas. Most of these hypotheses are explained in terms of nucleation and growth [24, 26, 27], nucleation catalysis [25], pore development [28, 29], mechanistic and structural aspects [30, 31], as well as the time and temperature dependence [32, 33].

Generally, the hydroxides of aluminium and its derivatives are dehydrated topotactically (i.e. the crystal structure transforms without destruction of the original crystal morphology) and occurs at about 450° C to form γ-Al_2O_3 having a well-defined pore structure [16, 26]. With further heating, transformation to other transitional alumina phases such as δ- and θ-alumina also occurs topotactically and with changes in the pore structure to accommodate densification. Finally, α-alumina forms by a nucleation and growth process [16, 26, 27, 33] at around 1200° C. The major difference between these metastable aluminas is the degree of ordering of the oxygen lattice in their cell structures.

From the results obtained in this investigation, the sequence of phase transformations in alumina gels is obviously quite different from those mentioned above. The γ- and θ-aluminas are the only intermediates formed prior to the formation of corundum at about 1200° C. The γ-alumina has an extremely fine crystallite size, of the order ~ 5 nm (Fig. 6). This phase has been well established to possess a cubic spinel structure cell with tetrahedral aluminium lattice strongly disordered but the oxygen lattice is fairly well ordered [16]. Cation vacancies are randomly distributed between octahedrally coordinated sites and they arise from the necessity to maintain charge balance. The lattice structure of θ-alumina differs from γ-alumina only in the number of aluminium ions occupying tetrahedral and octahedral holes in an approximately cubic closest packing of O^{2-} ions [34]. On the contrary, the α-alumina belongs to the corundum-type structure where aluminium cations occupy two-thirds of the octahedral sites in a hexagonal oxygen lattice. The octahedra are joined to form a chain perpendicular to the oxygen layers, every third site being empty. The octahedral cation positions can be easily occupied by aluminium ions, whereas the tetrahedral sites are inaccessible to these ions [35].

The formation of α-alumina from γ-alumina would inevitably involve the initial ordering of oxygen lattice to form θ-alumina and the subsequent rearrangement of the oxygen lattice from a more or less distorted cubic array to a hexagonal close packed structure, together with a change in the coordination of those cations which previously occupied tetrahedral sites to octahedral sites and an increasing ordering of the cation vacancies. This mechanism of formation in a gel has been proposed to occur by a nucleation and growth process [27]. The transformation involves the formation and growth of spherical colonies of α-alumina in a porous matrix of submicrometre γ-alumina (~ 5 nm). Within the colonies, the α-alumina is interconnected with a continuous pore phase. The entire colony behaves as a single crystal of α-alumina which grows gradually via a coarsening process to reduce the surface area and crystal defects. After

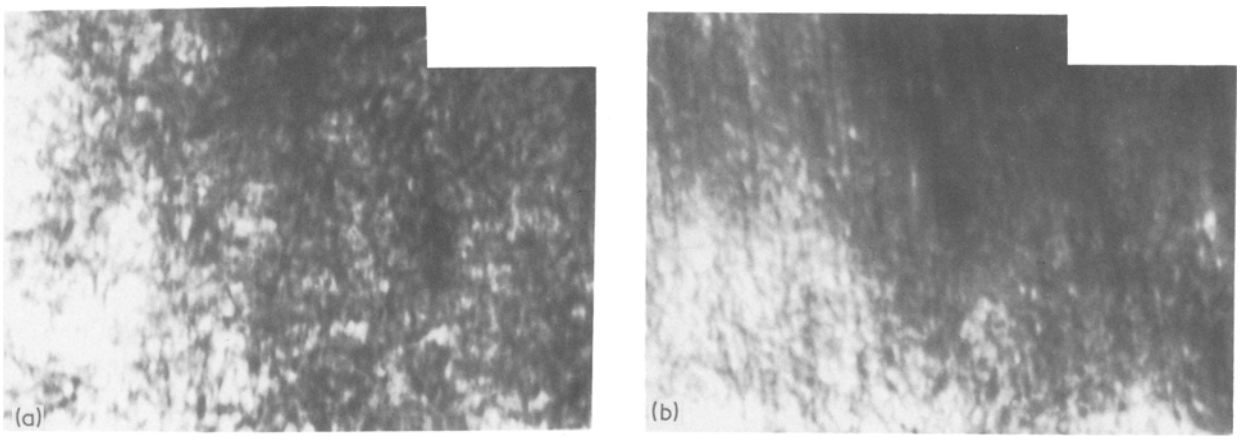

Figure 6 Electron micrograph of alumina gel treated (a) at the ambient temperature and (b) at 600° C, × 187 500.

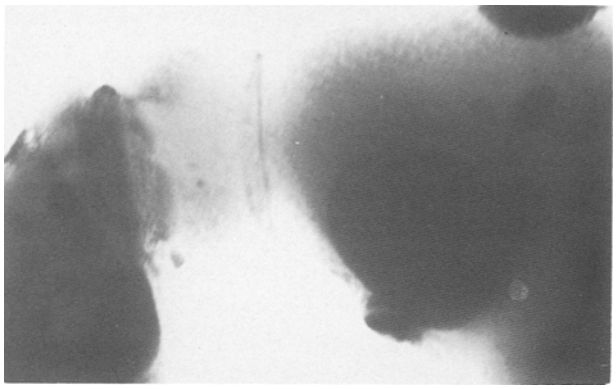

Figure 7 Electron micrograph of Al_2O_3 + 8 wt % ZrO_2 treated at 1300° C, × 200 000

complete transformation to α-alumina, the microstructure consists of a vermicular network in which both the pore and solid phase are contiguous and the pore channels are of the same scale as the α-alumina grains [33].

4.2. Formation of solid solutions between zirconia and alumina

The lack of published values on the solid solubility of zirconia in alumina renders the verification of the value obtained in this study almost impossible. However, alumina has been found in nature to form limited solid solutions with chromium oxide, titanium oxide and magnesia to form ruby, blue sapphire and yellow sapphire, respectively. Other oxides such as Fe_2O_3, SiO_2 or NiO are often found associated with pure alumina as minerals. Kennedy and Bradt [36] reported a solution of up to 2 mol % $MgO \cdot TiO_2$ in alumina. Because of the relatively large ionic radius of the zirconium atom, only a limited amount of zirconia can be incorporated into the structure of alumina to form a solid solution. The value of 1.85 wt % (~ 1.5 mol %) at 1300° C obtained in this study may be treated as generally correct. As in the mullite–zirconia [19] system, the formation of solid solutions between zirconia and alumina at the range of temperatures studied is non-equilibrium.

Similar mechanisms of solid solution formation are believed to be operating in alumina–zirconia ceramics as in the composites of mullite–zirconia [19]. The variation of corundum cell dimensions with the amount of zirconia added (Fig. 1) suggest that up to 1.85 wt % zirconia may be incorporated to form a metastable solid solution at 1300° C. Only a fraction of this amount is believed to have entered the corundum structure via substitution for aluminium atoms at the octahedral sites because of the relatively large zirconium ions which are expected to appear only in octahedral coordination as in the mullite–zirconia system. The majority of zirconium atoms are postulated to have resided metastably at the interstices and vacancy domains. The apparent higher value of solid solubility of zirconia obtained for alumina–zirconia ceramics as compared to 0.9 wt % in mullite–zirconia ceramics [19] at the same temperature remains enigmatic. However, in terms of mole percentage, the solid solubility of ZrO_2 in alumina (~ 1.5 mol %) at 1300° C is, in fact, smaller than that in mullite (~ 3 mol %)! Maximum solubility of zirconia (~ 5 wt % or ~ 4 mol %) is expected to occur in γ-alumina, a cubic spinel with considerable amount of defects and disorder. In addition, this cubic spinel also displays some degree of pronounced tetragonal character [16] which may serve to enhance the mechanism of solid solution formation via the phenomenon of krypto-isomorphism with tetragonal zirconia. The decreasing of this value with increasing temperatures and heating times is probably due to "de-stuffing" of zirconium atoms which were metastably located at interstices and vacancy domains.

The above hypothesis is substantiated by the results obtained for the variation of the *c*-dimension of corundum with the amount of zirconia introduced. This dimension appeared to vary very little while the largest variation occurred in the *a*-dimension. This observation serves to suggest that only a very limited number of zirconium atoms have substituted for aluminium atoms at the octahedral chains and while most of them are "stuffed" at the interstices and vacancy domains to cause large expansion of the lattice in the *a*-axis.

4.3. The effect of dispersed zirconia particles on the microstructural developments in alumina ceramics

As in mullite–zirconia ceramics, addition of zirconia in the amount which forms a solid solution with corundum tends to accelerate the grain-coarsening process (Fig. 4). Apparently, when present in solid solution, zirconia inclusions enhance the lattice diffusion and the rate of boundary migration which are essential for Ostwald ripening. It follows that zirconia may function as an excellent solid solution sintering aid for alumina ceramics.

The apparent absence of grain refinement in the alumina–zirconia ceramics at temperatures up to 1400° C is in contradiction to the observations reported by several investigators. Lange and Hirlinger [10] and Green [11] observed a grain refinement of corundum for compositions containing zirconia greater than 5 and 7.5 vol %, respectively. The former attributed the grain-growth control to the dragging force exerted by the zirconia inclusions at the four-grain junctions which subsequently suppressed the grain growth. They also reported that these inclusions in alumina matrix have enough self diffusivity to show the same behaviour as the pores except that the inclusions do not disappear. Abnormal grain growth was thought to be the result of non-uniform distribution of inclusions in the microstructure to hinder the growth of all alumina grains. Pinning of alumina grain boundaries by the zirconia particles was believed by Green [11] to be responsible for limiting the alumina grain growth. The limiting grain size was found to be dependent on the size and volume fraction of zirconia inclusions. In addition to zirconia, MgO has been widely used as a grain-refining agent for alumina ceramics [37–39].

The absence of observable grain refinement in this study may be due to the inherent microporous texture of the alumina gel which persisted even when heat

treated at high temperatures (Fig. 6). It is well established that gels contain numerous submicroscopic pores [16] which are difficult to eradicate by means of heat treatment. These pores are believed to be responsible for the overall reduction on the rate of lattice diffusion and boundary migration. The latter is reflected in the surface-diffusion controlled pore drag which can effectively suppress the mechanisms of grain coarsening.

The mobility of pores may be presented by $M_p = K'(D_s/r^4)$ [40], where D_s is the surface diffusion coefficient, K' a constant and r the radius of a spherical pore. The phenomenon of pore-boundary attachment is particularly favourable in a microstructure with fine grain size and large (M_p/M_b) ratio where M_b is the boundary mobility. If the size of corundum grains in the composites is assumed to be twice as large as those in the pure alumina system and that the pore size $(2r)$ is proportional to the grain size, then, $r^* > r/2$ and $M_p > 16\,M_p^*$, where r^* and M_p^* represent parameters associated with alumina grains doped with zirconia. As $M_b^* > M_b$ [37], it follows that $(M_p/M_b) > 16\,(M_p/M_b)^*$. Therefore, the high susceptibility of pore-boundary attachment in microporous alumina gel is established and it is this interaction of pores with boundaries which is believed to give rise to the observed fine microstructure and its persistence at high temperatures. It is anticipated that the grain refinement of alumina–zirconia composites may only be exhibited at very high temperatures where the porous structure and hence the pore dragging in the alumina system is removed so that rapid grain coarsening can occur. Under these conditions, the pore-boundary interaction would be insignificant compared with the dragging force exerted by the inclusions and the above model for grain-growth inhibition may be applicable by replacing pores with inclusions. However, addition of zirconia in excess may inhibit sintering and drastically increase the total porosity and mean pore size [41], allowing the phenomenon of pore-boundary attachment, mentioned above, to operate again. The model derived above is applicable for all heterogeneous microstructures. In microporous structures, pores are second phases while in non-porous microstructures, inclusions are second phases responsible for interacting with the grain boundaries. As pointed out by Lang and Hirlbinger [10], inclusions can behave like pores and vice versa except that pores tend to disappear at high temperatures while inclusions do not. By computing the effect of MgO solute on the kinetics of grain growth in Al_2O_3, Bennison and Harmer [37] showed that MgO acts to increase the mobility ratio, M_p/M_b by a factor of 80, an amount sufficient to favour pore-boundary attachment. It follows therefore that in microstructure which contains both pores and inclusions, the grain growth is initially limited by pore dragging with a transition towards limitation by inclusion dragging at high temperatures where pores are eliminated. The grain refinement observed in the literature is probably the result of very high temperature ($> 1600°$ C) treatment which caused pores in the microstructure to collapse and allowed undoped corundum grains to grow rapidly because of the absence of pore–boundary interaction. Similarly, the grain refinement observed for doped corundum could be attributed to the predominant inclusion dragging mechanism.

Besides controlling the microstructural developments of alumina ceramics, the presence of metal ions in solid solution with Al_2O_3 has been found to alter the kinetics of alumina phase transformations. Lippens and De Boer [16] reported that the occupation of octahedral sites in Al_2O_3 by sodium ions can prevent the ordering of γ-Al_2O_3 into the δ-Al_2O_3, resulting in the stabilization of θ-Al_2O_3. On the other hand, the presence of magnesium, nickel or lithium ions which occupy tetrahedral sites tends to favour formation of δ-Al_2O_3 [17]. The role of zirconium on the sequence of alumina phase transformations is unclear in this investigation, although a similar mechanism is anticipated.

A perusal of the crystallization temperature of corundum in Table I suggests that the transformation of transitional aluminas to corundum may be enhanced by the addition of zirconia. This observation is also reported by numerous workers. For instance, Suwa *et al.* [42] seeded Al_2O_3–MgO gels with α-Al_2O_3, $MgAl_2O_4$, α-Fe_2O_3 and SiO_2 to study the extent of nucleation catalysis of solid state reactions. Seeding with α-Al_2O_3 was observed to lower the α-Al_2O_3 crystallization temperature in these gels by 100 to 150° C. Spinel seeds had much less effect on the $\gamma \rightarrow \alpha$ transition, and α-Fe_2O_3 and SiO_2 did not affect it significantly. It appears that isostructural seeding of gels may permit lower ceramic processing temperatures. Wakao and Hibino [43] added a number of oxides up to 10 wt % to an aluminium sulphate derived α-Al_2O_3 and reported that the temperature of the θ- to α-Al_2O_3 transformation was reduced in all cases, with CuO and Fe_2O_3 lowering the transformation temperature to as low as 1050° C. Similar observation was also reported elsewhere [33].

5. Conclusions

The crystallization behaviour of alumina and alumina–zirconia ceramics has been investigated. The phase transformations of alumina gel to corundum involves the formation of γ- and θ-Al_2O_3 as intermediates. The presence of zirconia tends to enhance the conversion of metastable aluminas to corundum.

Zirconia forms a metastable solid solution with aluminas. The extent of solid solution is greater than 5 wt % (~ 4 mol %) ZrO_2 in γ-Al_2O_3 while it is less than 2 wt % (~ 1.7 mol %) in corundum at 1300° C. When present in solid solution, zirconia enhances rapid growth of corundum grains. In contradiction to observations reported in the literature, there is no apparent grain refinement in alumina–zirconia composites with respect to the pure alumina system. The fine microstructures obtained have been shown to be related to the microporous texture of gel structures which allow the interaction of pores and boundaries to result in the overall reduction of the rate of lattice diffusion and boundary migration. It is anticipated that the grain refinement in these composites will become evident only at high temperatures ($> 1500°$ C)

where pores and hence pore dragging forces are eliminated, allowing the mechanism of inclusion (ZrO_2) dragging to be exemplified.

Acknowledgements

We thank Monash University for the financial assistance in the form of a scholarship to one of us (I.M.L.).

References

1. H. P. ROOKSBY, in "The X-ray Identification and Crystal Structure of Clay Minerals", edited by G. Brown (Mineral. Society, London, 1961) pp. 345–92.
2. R. McPHERSON, *J. Mater. Sci.* **8** (1973) 859.
3. M. S. G. GANI and R. McPHERSON, *ibid.* **12** (1977) 999.
4. P. F. BECHER, *J. Amer. Ceram. Soc.* **64** (1981) 37.
5. N. CLAUSSEN, *ibid.* **59** (1976) 49.
6. N. CLAUSSEN, J. STEEB and R. PABST, *Bull. Amer. Ceram. Soc.* **56** (1977) 559.
7. J. STEVEN and G. EVANS, *Br. Ceram. Trans. J.* **83** (1984) 28.
8. E. P. BUTLER and A. H. HEUER, *Commun. Amer. Ceram. Soc.* **65** (1982) C206.
9. P. F. BECHER, *J. Amer. Ceram. Soc.* **66** (1983) 485–88.
10. F. F. LANG and M. M. HIRLINGER, *ibid.* **67** (1984) 164.
11. D. J. GREEN, *ibid.* **65** (1982) 610.
12. S. HORI, M. YOSHIMURA and S. SOMIYA, in "Zirconia Ceramics", edited by S. Somiya and K. Uchida (Rokakuho, Tokyo, 1983) 1–7.
13. S. HORI, R. KURITA, M. YOSHIMURA and S. SOMIYA, *J. Mater. Sci. Lett.*, in press.
14. M. YOSHIMURA, S. KIKUYAWA and S. SOMIYA, *J. Jpn Ceram. Soc.* **91** (1983) 51.
15. N. CLAUSSEN, G. LINDEMANN and G. PETZOW, *Ceram. Int.* **9** (1983) 83.
16. B. C. LIPPENS and J. H. DE BOER, *Acta. Crystallogr.* **17** (1964) 1312.
17. A. M. LEJUS and R. C. COLLONGUES, "Proceedings of the 5th International Conference on Reactivity of Solids", edited by Schwab (Elsevier, Amsterdam, 1965) pp. 373–9.
18. G. C. WHITAKER, *Adv. Chem. Ser.* **23** (1957) 184.
19. I. M. LOW, PhD thesis, Monash University, Australia, 1986.
20. I. M. LOW and R. McPHERSON, Proceedings of the 11th Australian Ceramic Society Conference (1984) pp. 471–4.
21. B. E. YOLDAS, *Bull. Amer. Ceram. Soc.* **54** (1975) 289.
22. P. TARTE, *Silicate Ind.* **28** (1963) 345.
23. S. KOMARNENI and R. ROY, *J. Amer. Ceram. Soc.* **68** (1985) C243.
24. B. E. YOLDAS, *J. Appl. Chem. Biotech.* **23** (1973) 803.
25. M. KUMAGAI and G. L. MESSING, *J. Amer. Ceram. Soc.* **68** (1985) 500.
26. S. J. WILSON, *J. Solid State Chem.* **30** (1979) 247.
27. F. W. DYNYS and J. W. HALLORAN, *J. Amer. Ceram. Soc.* **65** (1982) 442.
28. R. K. ILLER, *ibid.* **44** (1961) 618.
29. S. J. WILSON, *Mineral. Mag.* **43** (1979) 301.
30. *Idem, Proc. Br. Ceram. Soc.* **28** (1979) 281.
31. S. J. WILSON and M. H. STACEY, *J. Colloid Interface Sci.* **82** (1981) 507.
32. S. J. WILSON and K. McCONNELL, *J. Solid State Chem.* **34** (1980) 315.
33. F. W. DYNYS and J. W. HALLORAN, "Ultrafine Processing of Ceramics, Glasses and Composites", edited by L. L. Hench and D. R. Ulrich (Wiley, New York, 1984) pp. 242–51.
34. A. F. WELLS, "Structural Inorganic Chemistry", 4th Edn (Clarendon, Oxford, 1975) pp. 450–3.
35. J. NEDOMA, *Zesz. Nauk. Akad. Gorn. -hutu. Krakow* **22** (1973) 7.
36. C. R. KENNEDY and R. C. BRADT, *J. Amer. Ceram. Soc.* **56** (1973) 608.
37. S. J. BENNISON and M. P. HARMER, *ibid.* **66** (1983) C90.
38. A. MOCELLIN and W. D. KINGERY, *ibid.* **56** (1973) 309.
39. M. P. HARMER, E. W. ROBERTS and R. J. BROOK, *Trans. J. Br. Ceram. Soc.* **78** (1979) 22.
40. R. J. BROOK, Treatise on Materials Science and Technology, Vol. 9, edited by F. F. Y. Wang (Academic, 1976) pp. 331–64.
41. C. BAUDIN and J. S. MOYA, *J. Amer. Ceram. Soc.* **67** (1984) C134.
42. Y. SUWA, R. ROY and S. KOMARNENI, *ibid.* **68** (1985) C238.
43. Y. WAKAO and T. HIBINO, *J. Jpn Ceram. Soc.* **11** (1962) 588.

Received 8 December 1987
and accepted 13 May 1988